# Anomalous magnetic moments as evidence of chiral superconductivity in a Bi/Ni bilayer

Junhua Wang,[1] Xinxin Gong,[2] Guang Yang,[1] Zhaozheng Lyu,[1] Yuan Pang,[1] Guangtong Liu,[1] Zhongqing Ji,[1] Jie Fan,[1] Xiunian Jing,[1,3] Changli Yang,[1,3] Fanming Qu,[1] Xiaofeng Jin,[2,*] and Li Lu[1,3,*]

[1]*Beijing National Laboratory for Condensed Matter Physics, Institute of Physics, Chinese Academy of Sciences and School of Physical Sciences, University of Chinese Academy of Sciences, Beijing 100190, People's Republic of China*

[2]*State Key Laboratory of Surface Physics and Department of Physics, Fudan University, Shanghai 200433, People's Republic of China*

[3]*Collaborative Innovation Center of Quantum Matter, Beijing 100871, People's Republic of China*

(Received 9 November 2016; revised manuscript received 30 July 2017; published 28 August 2017)

There have been continuous efforts in searching for unconventional superconductivity in the past five decades. Compared to the well-established $d$-wave superconductivity in cuprates, the existence of superconductivity with pairing symmetries of other high angular momentum is less conclusive. Bi/Ni epitaxial bilayer is a potential unconventional superconductor with broken time reversal symmetry (TRS), for that it demonstrates superconductivity and ferromagnetism simultaneously at low temperatures. We employ a specially designed superconducting quantum interference device (SQUID) to detect, on the Bi/Ni bilayer, the orbital magnetic moments which are expected if the TRS is broken. An anomalous hysteretic magnetic response is indeed observed in the superconducting state, providing the evidence for the existence of chiral superconducting domains in the material.

DOI: 10.1103/PhysRevB.96.054519

In searching for unconventional superconductivity with broken TRS, it was proposed that spin triplet pairing could be triggered by magnetic fluctuations in ferromagnetic metals [1–3], with shared itinerant electrons responsible for both superconductivity and ferromagnetism [4,5]. The coexistence of superconductivity and ferromagnetism at low temperatures has been reported in $UGe_2$ [6], URhGe [7], and UCoGe [8]. Spin triplet pairing was believed also to occur via proximity effect at the interface between $s$-wave superconductor and ferromagnetic metal [9,10]. The existence of a supercurrent across a NbTiN-$CrO_2$-NbTiN junction was regarded as the evidence [11]. The most extensively studied candidate of chiral $p$-wave superconductor is probably $Sr_2RuO_4$ [12–14], with which anomalous responses in phase sensitive experiments [15–17] and the appearance of half flux quantum [18] have been observed. However, the existence of domain-edge current, a signature for chiral superconductivity due to broken TRS, has not yet been confirmed [19–21].

As a potential unconventional superconductor, Bi/Ni bilayer film was first studied by Moodera and Meservey [22] and later by LeClair and coworkers [23]. Superconductivity was observed to coexist with ferromagnetism below $T_c = 4.2$ K and was thought to originate from a possible *fcc*-structured Bi on *fcc*-structured Ni [23]. Recently, Gong and coworkers further revealed the coexistence of superconductivity and ferromagnetism in an epitaxial form of Bi/Ni bilayer which contains only ordinary rhombohedra instead of *fcc*-structured Bi [24,25]. Since neither rhombohedra Bi nor *fcc* Ni is superconducting individually at the temperatures explored, the superconductivity is possibly triggered by magnetic fluctuation at the interface and hence likely to be unconventional [1,24,25].

If the superconductivity in Bi/Ni bilayer is indeed unconventional and contains chiral superconducting domains due to broken TRS, there will be observable out-of-plane magnetic moments at the edges [Fig. 1(a)], due to the positional mismatch (hence the incomplete cancellation) between the outmost domain-edge current and the inward Meissner screening supercurrent [26]. In this work, we have constructed SQUIDs in such a way that a portion of the interference loop is based on the Bi/Ni bilayer itself [Fig. 2(a)]. This configuration is most sensitive for exploring edge magnetization—any variation in edge magnetization will directly change the total flux in the SQUID loop [Fig. 1(b)]. We have indeed observed an anomalous hysteretic interference pattern on such SQUIDs. We attribute the hysteresis to the motion of chiral superconducting domains on the bilayer.

The SQUIDs we used contain two half rings, as shown in Fig. 2(a). One half ring is etched off from the Bi/Ni bilayer, with a width of 1 $\mu$m and inner radii listed in Table I. The Bi/Ni bilayer contains 2-nm-thick *fcc*-structured Ni and 30-nm-thick rhombohedra-structured Bi, grown sequentially on MgO substrate via molecular beam epitaxy [24]. The other half ring is made of superconducting Pb film, which is 50 nm thick and with a width of 1.4 $\mu$m. Au film pads of 30 nm thick are sandwiched between the two half rings. The strong superconducting proximity effect between Pb and Au film guarantees Josephson couplings between the two half rings up to a distance of $>0.5$ $\mu$m. We note that the use of a Pb half ring is necessary, because the superconducting proximity effect between Bi/Ni and Au is not strong enough to mediate Josephson supercurrents through Bi/Ni-Au-Bi/Ni junctions.

Six such SQUIDs were investigated at a temperature of $\sim$30 mK provided by dilution refrigerators. The differential resistance $dV/dI_b$ of the devices was measured as a function of bias current $I_b$ and out-of-plane magnetic fields $H$ by using lock-in amplifier techniques. Roughly periodic interference patterns were observed for all devices. A typical such pattern in unidirectional magnetic field sweepings is shown in Fig. 2(b). The period of the oscillations is $\Delta B = 0.55 \pm 0.03$ Oe, which is in excellent agreement with the loop area of the device,

*Corresponding authors: lilu@iphy.ac.cn, xfjin@fudan.edu.cn

 

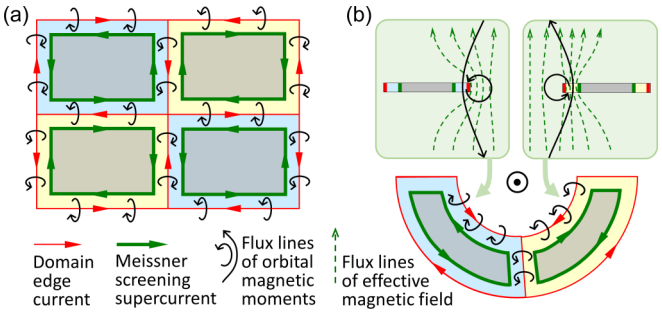


FIG. 1. Cartoon pictures of chiral superconducting domains. (a) Illustration of the edge currents, the Meissner screening supercurrents, and the magnetic flux lines of the unscreened orbital magnetic moments near the edge of the domains. The domains with different chirality are illustrated in different color. (b) (Lower panel) A half ring of chiral superconductor containing two superconducting domains of opposite chirality. (Upper panel) Cross-section views of the magnetic flux lines at the inner edge of the half ring in an applied magnetic field.

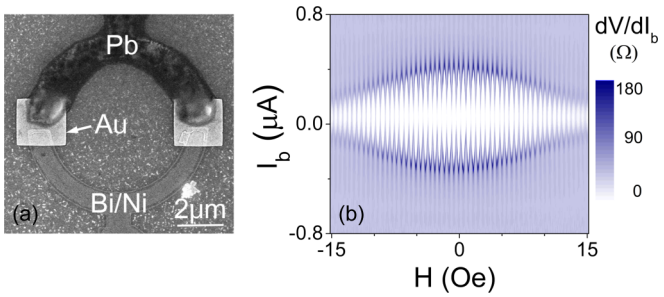


FIG. 2. A typical Pb-Bi/Ni SQUID and its interference pattern. (a) Scanning electron microscope image of device #1. The upper half ring is made of Pb film, and the lower half ring is made of Bi/Ni epitaxial bilayer. They are connected by two squarelike Au films through a superconducting proximity effect at low temperatures. The whitish structures at the edge of the Bi/Ni half ring are the residual PMMA which is difficult to lift off after reactive ion etching. (b) 2D plot of differential resistance $dV/dI_b$ as a function of out-of-plane magnetic field and bias current at $T = 30$ mK.

$A_{loop} = 39.3\ \mu m^2$, via the relation $A_{loop}\Delta H = \phi_0$ (where $\phi_0$ is the flux quantum).

However, we noticed that the device enters into a transient state whenever the sweep direction of magnetic field is reversed. The oscillation period is compressed in this transient state. Figure 3(a) shows the $dV/dI_b$ oscillation patterns in two sweep circles, measured on device #1 at $I_b = 0$. Let us first look at the green trace which was measured by sweeping the field from the right to the left. The oscillation period is compressed at the beginning, then gradually recovers to the normal value (entering into a stable state). The range of the transient state $H_t$ is marked by the light-green color bar at the top. Once the sweep direction is reversed from the left to the right (i.e., the red trace), the oscillation period is compressed again at the beginning, then gradually recovers to the normal value again.

In Fig. 3(a), we also show a smaller sweep circle containing the blue trace and the black trace. Similar transient states exist, with about the same length of $H_t$ compared to that on the green and the red traces. After having passed the transient states and entered into the stable state, e.g., in region A for the negative field sweep direction and in region B for the positive field sweep direction, the peak positions on traces of the same sweep directions overlap with each other.

Due to the compression in the transient states, however, the peaks with the same indexes but on traces of opposite sweep directions are shifted with each other, as shown in Fig. 3(b). Here we note that the peaks on the two traces of a closing sweep circle are one-to-one correlated and are indexed from the left to the right. The shift is "advanced" with regard to the field sweep direction, such that a given indexed peak occurs before reaching its position on the trace of opposite sweep direction. This is the main discovery of this experiment.

There are two additional features to be mentioned. One is that the occurrence or not of the hysteresis is independent of the strength of the magnetic field. For example, a hysteretic circle can occur in entirely negative fields [Fig. 3(c)] or in entirely positive fields, as well as in a region between negative and positive fields. The other feature is that, on the traces of same field sweep direction, the peak positions in both the transient state and the stable state are independent of the field sweep rate. This can be readily seen from Fig. 3(d). More data taken at different sweep rates can be found in the Supplemental Material [27].

The observed anomalous hysteresis, appearing to be "advanced" and occurring at any magnetic field once the sweep direction is reversed, is very different from the ordinary hysteresis caused by domain wall motion in ferromagnetic materials or by flux pinning in superconductors. It should be noted that there is no flux pinning in our devices, since the maximal out-of-plane magnetic field is kept well below 20 Oe during the measurements, being insufficient to create a vortex on the Bi/Ni strip of 1 $\mu$m in width. The anomalous hysteresis is also unlikely caused by the instrumental delay during data acquisition. In fact, the amount of hysteresis is unchanged even if the sweep rate is varied by three orders of magnitude [27]. In addition, the SQUIDs are not in the hysteretic regime, since the SQUID screening parameter $\beta_e = 2\pi L I_c/\phi_0$ is much smaller than 1 (where $L \approx 6$ pH is the inductance of the SQUID loop, and $I_c < 1\ \mu$A is the critical supercurrent) [28]. All these inferences are further supported by our control experiment on conventional Pb-Au-Pb SQUIDs, in which no hysteresis can be recognized [27].

To quantitatively analyze the hysteretic behavior, we collected a hysteresis circle of $dV/dI_b$ on device #2 at $I_b = 0.5\ \mu$A. The result is shown in Fig. 4(a). The oscillations of $dV/dI_b$ are caused by the oscillations of $I_c$, the critical supercurrent of the SQUID which has the form of [28]:

$$I_c \propto \cos\left[2\pi\frac{(H - H_0)A_{loop}}{\phi_0} + \delta\right], \quad (1)$$

where $H_0$ is a small constant caused by, e.g., the earth magnetic field. $\delta$ is the accumulated anomalous phase shift counted from the point where the sweep direction is reversed. The phase change between neighboring $dV/dI_b$ peaks must satisfy:

$$2\pi\frac{\Delta H_n A_{loop}}{\phi_0} + \Delta\delta_n = 2\pi, \quad (2)$$

TABLE I. A list of the parameters of six devices investigated.

| Device | Distance[a] ($\mu$m) | Inner Radius ($\mu$m) | Loop Area ($\mu$m$^2$) | Calculated Period (Oe) | Measured Period (Oe) | $2\delta_0/2\pi$ |
|---|---|---|---|---|---|---|
| #1 | 0.4 | 3.0 | 39.3 | 0.53 | 0.55 ± 0.03 | 2.89 ± 0.01 |
| #2 | 0.5 | 1.0 | 6.2 | 3.34 | 3.37 ± 0.06 | 0.54 ± 0.04 |
| #3 | 0.2 | 1.0 | 6.1 | 3.39 | 3.13 ± 0.08 | 0.70 ± 0.04 |
| #4 | −0.4 | 1.0 | 5.6 | 3.69 | 3.5 ± 0.2 | 0.60 ± 0.07 |
| #5 | −0.4 | 2.0 | 17.6 | 1.18 | 1.12 ± 0.09 | 1.7 ± 0.2 |
| #6 | −0.4 | 3.0 | 35.9 | 0.59 | 0.58 ± 0.03 | 2.7 ± 0.2 |

[a]The lateral distance between Pb and Bi/Ni at the junctions. A negative value denotes the overlap of the two half rings.

where $\Delta H_n$ is the field interval between the neighboring $dV/dI_b$ peaks of indexes $n$ and $n+1$, as illustrated in Fig. 4(a) and plotted in Fig. 4(b), and $\Delta\delta_n$ is the difference of $\delta$ between the neighboring peaks of indexes $n$ and $n+1$.

By using Eq. (2) and the data of $\Delta H_n$ shown in Fig. 4(b), $\Delta\delta_n$ can be calculated. The accumulated anomalous phase shift $\delta$ can be further obtained by adding up $\Delta\delta_n$. The results are shown in Fig. 4(c). It can be seen that, after having passed the transient states, the accumulated anomalous phase shift $\delta$ saturates to $\delta_0$ or $-\delta_0$ as represented by the two dashed lines in Fig. 4(c). Once the sweep direction is reversed, $\delta$ immediately starts to chase the other saturated state, resulting in the observed "advanced" nature.

Such an anomalous hysteresis is in sharp contrast to that of ferromagnetic domain-wall motion. Therefore, it should be irrelevant to the ferromagnetic moment of the Ni layer. To further support this argument, we applied a magnetic field up to 1000 Oe in the in-plane direction of the bilayer, to drive the Ni layer into a single domain and at the same time to fully fix the direction of its ferromagnetic moment. According to earlier studies [24], the ferromagnetic moment of the Ni layer becomes saturated above 100 Oe. We find that the amount of anomalous phase shift between the two saturated states in out-of-plane magnetic field sweepings, $2\delta_0$, keeps unchanged with varying in-plane magnetic fields. The results are shown in Figs. 5(a) to 5(e). It confirms that the anomalous hysteresis is indeed irrelevant to the ferromagnetic moment of the itinerant electrons in Ni.

At a first glance, it is puzzling why the hysteretic dynamics starts immediately upon the reversal of field sweeping direction, showing the "advanced" instead of a retarded nature, and why the occurrence of saturated state is independent of the field strength. These features are different from the ordinary hysteretic behavior seen in ferromagnetic materials due to ferromagnetic domain-wall motion and are also different from that seen in superconductors due to flux motion/pinning.

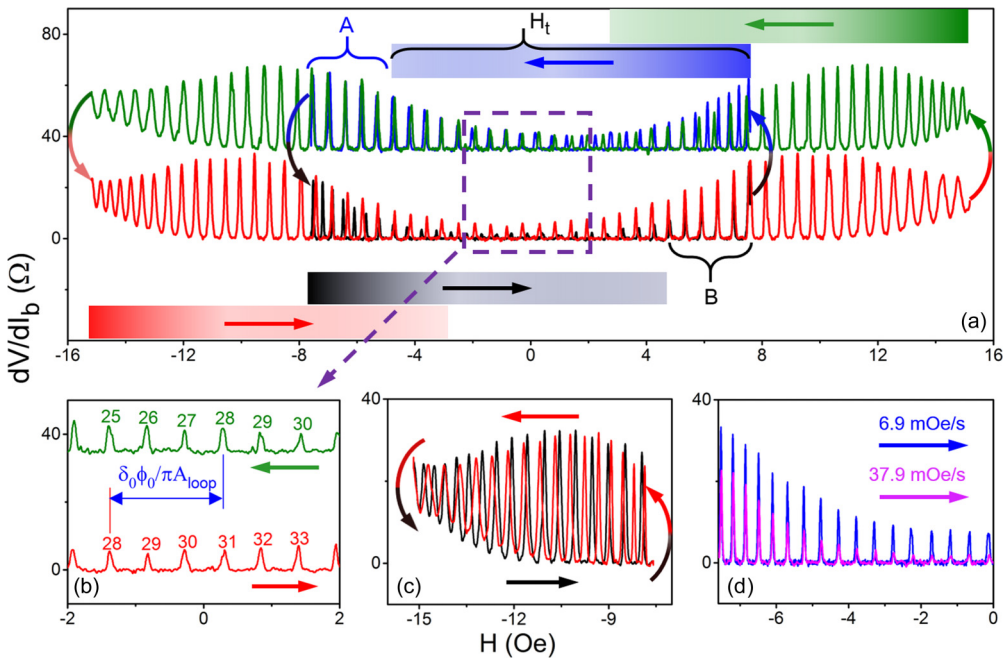


FIG. 3. Anomalous hysteresis in superconducting interference pattern during bidirectional field sweepings. (a) $dV/dI_b$ of device #1 measured at $I_b = 0$ and with an ac excitation current of 0.01 $\mu$A at $T = 30$ mK. The traces with green and blue colors are shifted vertically for clarity. The arrows indicate the sweep directions, and the bars of length $H_t$ denote the regions of transient states within which the oscillation period is compressed. (b) The green and the red traces in their stable states. The peaks are indexed from the left side of the traces in (a). (c) A hysteretic circle can take place in entirely negative magnetic fields, not necessary surrounding zero field. (d) Along the same sweep direction, the peaks on traces of different sweep rates align with each other.

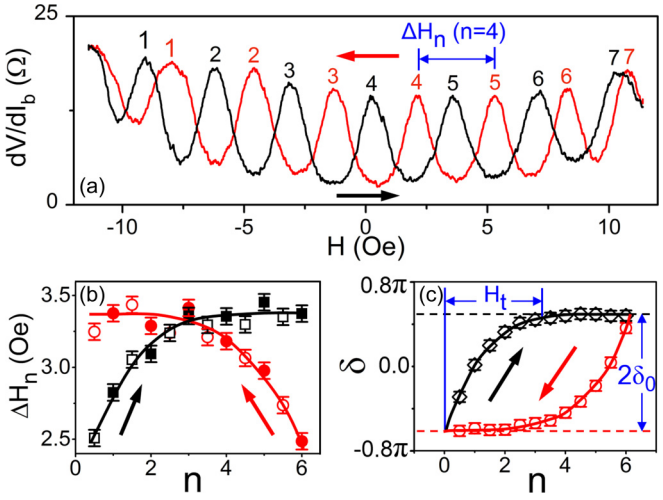


FIG. 4. More data obtained on another device. (a) Anomalous hysteresis of $dV/dI_b$ measured on device #2, with $I_b = 0.5$ $\mu$A and an ac excitation current of 0.05 $\mu$A at $T = 30$ mK. The peaks are indexed from the left of this sweeping circle. (b) The local period $\Delta H_n$ between neighboring peaks (valleys) of indexes $n$ $(n - 0.5)$ and $n + 1$ $(n + 0.5)$ is plotted against $n$ as solid (open) symbols. (c) The accumulated anomalous phase shift $\delta$. After having passed the transient states, $\delta$ reaches the saturated values as represented by the dashed black and red lines.

To understand these puzzles, we recall that an "advanced" hysteretic Fraunhofer pattern was observed in $Sr_2RuO_4$-Cu-Pb Josephson junctions by Kidwingira and coworkers [16,17]. There the phenomenon was interpreted as the motion of superconducting domain walls. We find that the same scenario is applicable to the phenomenon observed here. By assuming the existence of chiral superconducting domains,

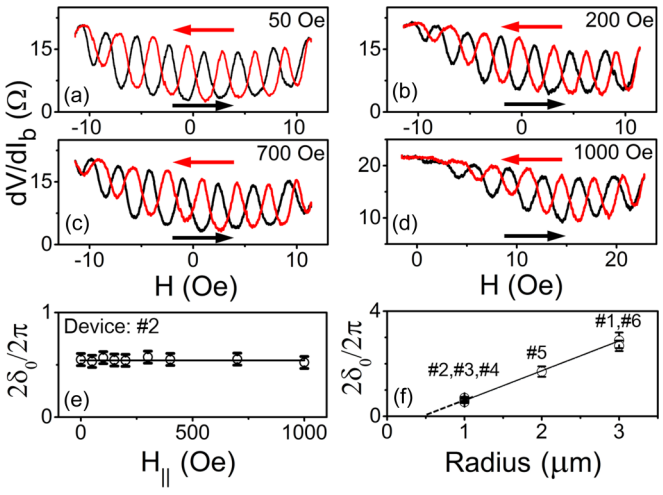


FIG. 5. The parallel magnetic field and the device size dependences of the anomalous phase shift. (a)–(d) Hysteresis of $dV/dI_b$ measured on device #2 at in-plane magnetic fields of $H_{\|} = 50$, 200, 700, and 1000 Oe, respectively. The horizontal shift of the envelope is mainly caused by the out-of-plane component of the magnetic field. (e) $H_{\|}$ dependence of $2\delta_0/2\pi$. (f) $2\delta_0/2\pi$ of six devices plotted as a function of the inner radius of the Bi/Ni half ring.

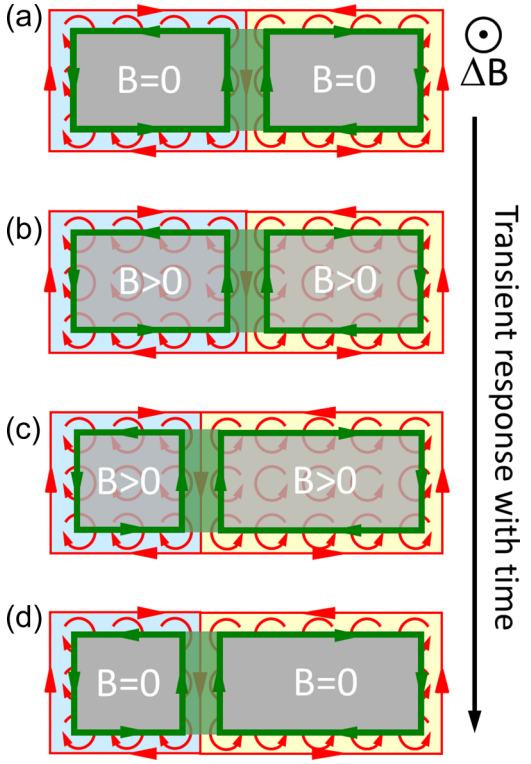


FIG. 6. The transient processes of superconducting domain-wall motion. (a) In the quasistatic state, the Cooper pairs in chiral superconducting domains feel zero neat magnetic field because of Meissner screening. The red circular arrows represent the Cooper pairs with orbital moments. (b),(c) When the applied magnetic field is varied, it takes a characteristic time of $\tau_{\text{Meissner}}$ for the Meissner screening supercurrent (in green) to respond. During this time window the Cooper pairs are exposed to a neat magnetic field $B$, so that those domains with Cooper pairs' orbital moments parallel to $B$ expand, and those with antiparallel moments shrink. (d) After the transient time window, the majority of the Cooper pairs feel zero neat field again, so that the system enters into the quasistatic state again.

all the anomalous features can be consistently explained. The following is our detailed explanation.

Let us begin with a chiral superconductor containing two superconducting domains in an applied magnetic field $H$. If $H$ keeps constant, the Cooper pairs (except for those near the edge) feel zero neat magnetic field $B$ due to Meissner screening. The system is therefore in a quasistatic state, as shown in Fig. 6(a). Now, let $H$ suddenly change by an amount; the Meissner screening supercurrent (MSS) will take a time of $\sim\tau_{\text{Meissner}}$ to response and to redistribute. The characteristic time $\tau_{\text{Meissner}}$ describes the inductive delay of the MSS which circulates along the edge of the Bi/Ni bilayer. $\tau_{\text{Meissner}}$ is proportional to the inductance and hence the area of the Bi/Ni bilayer. During this transient time window, the orbital moments of Cooper pairs in the entire bilayer are exposed to the neat field $B$, as shown in Fig. 6(b), so that those superconducting domains with orbital moments parallel to $B$ expand, and those with antiparallel moments shrink, as shown in Fig. 6(c). In the above analysis we have assumed that the response of domain-edge current (hence the redistribution of domain wall), which takes place at a characteristic time scale of $\tau_{\text{edge}}$, is

much faster than the response of MSS, i.e., $\tau_{\text{edge}} \ll \tau_{\text{Meissner}}$. This is because the area involved in domain-wall motion is much smaller than the entire area of the Bi/Ni bilayer. After the time window of $\tau_{\text{Meissner}}$, the change of applied magnetic field is fully compensated by the change of MSS, so that the majority of the Cooper pairs in Bi/Ni bilayer feels zero neat magnetic field again. Therefore, the domain wall motion stops and the Bi/Ni bilayer enters into the quasistatic state again [Fig. 6(d)].

Since the processes described above are triggered by the change of the field rather than by the field itself, they can happen at any field $H$ as long as there are orbital moments antiparallel to the neat field $B$. This explains why the hysteresis loops can occur in entirely positive or entirely negative field regions [see Fig. 3(c)], not necessary surrounding $H = 0$.

With the above picture we can also explain why the dynamic response starts immediately after the reversal of field sweeping, giving rise to the "advanced" nature of hysteresis. If we keep sweeping $H$ along one direction, all the orbital moments will eventually be aligned to that direction (the direction of the neat field $B$), entering into a saturated state represented by the black or the red horizontal line in Fig. 4(c). Then, if we reverse the field sweeping direction, the neat field $B$ changes sign. All the moments suddenly become antiparallel to the neat field $B$, so that domain wall motion starts over immediately, leading to the appeared "advanced" nature.

Unlike the majority of orbital moments inside the domain which feel only the neat field $B$, the orbital moments within the penetration depth $\lambda_{\text{L}}$ from the edges of Bi/Ni bilayer feel the applied magnetic field $H$. There is a difference in total energy when these moments near the edges are parallel or antiparallel to $H$. However, probably because the penetrated area is a tiny fraction, the total energy difference between the parallel and antiparallel edge situations appears to be small and insufficient to drive the domain wall to overcome a barrier to move. We believe that this is why the Bi/Ni bilayer stays at the quasistatic states while $H$ is fixed. Of course, such a picture is true only when the absolute field strength is small. At large field strength, which was not explored in our experiment because we wanted to avoid flux pinning, all the orbital moments must be aligned to the direction of the applied magnetic field (if the superconductivity could still survive).

In the above discussion we have assumed that the domain wall needs to overcome an energy barrier in order to move. This is true—otherwise the system would eventually become a single domain at any finite magnetic field. In fact, the area of an $M$-$H$ hysteretic loop represents the work done against dissipation during domain wall motion.

Up to now, our overall picture can be summarized as follows. It is known that the domain-edge current is distributed within a length scale of $\xi$ (the coherence length) from the edge, whereas the MSS is distributed within the penetration depth $\lambda_{\text{L}}$ from the edge. According to Sigrist and coworkers [26], these two current paths do not fully overlap with each other in space, so that the orbital magnetic moments of the Cooper pairs near the edges are not fully screened by the MSS. Those unscreened moments at the inner edge of the Bi/Ni half ring contribute an anomalous flux to the SQUID loop in addition to the flux of applied magnetic field, as illustrated in Fig. 1. The motion of domain wall varies the anomalous flux in the SQUID loop in a hysteretic way, leading to the anomalous interference pattern.

In our picture, the accumulated anomalous phase shift reaches $\pm\delta_0$ when the inner edge of the Bi/Ni half ring becomes fully polarized, i.e., becomes single domained. $\delta_0$ is proportional to the total orbital magnetic moments of the Cooper pairs in the area $S$ between the edge current and the Meissner screening supercurrent at the inner edge of the Bi/Ni half ring:

$$\begin{aligned}\delta_0 &\propto S \propto [\pi(R_{\text{in}} + \lambda_{\text{L}})^2 - \pi(R_{\text{in}} + \xi)^2]/2 \\ &\propto \pi(\lambda_{\text{L}} - \xi)R_{\text{in}}, \end{aligned} \tag{3}$$

where $R_{\text{in}}$ is the inner radius of the Bi/Ni half ring, and $\lambda_{\text{L}} - \xi$ is of the order of magnitude a hundred nanometers or so. This equation explains the linear radius dependence of $\delta_0$ shown in Fig. 5(f). The intercept of the linear dependence at the abscissa in Fig. 5(f), $\sim$0.5 $\mu$m, might reflect the typical size of the superconducting domains—below this size the Bi/Ni half ring becomes single domained, so that the domain edge overlaps with the ring edge and is pinned by the ring edge.

To summarize, we have employed a very sensitive device configuration to study the out-of-plane edge magnetization of the Bi/Ni bilayer in its superconducting state. An anomalous hysteretic behavior irrelevant to the ferromagnetism of Bi/Ni bilayer has been observed. We attribute the anomalous hysteresis to the motion of chiral superconducting domains in the bilayer. Our method could be generalized to identify chiral superconductivity in other materials.

We would like to thank Junya Feng for fruitful discussions. This work was supported by the MOST Grant Nos. 2016YFA0300601, 2015CB921402, 2009CB929101, and 2011CB921702, by NSFC Grant Nos. 91221203, 11174340, 11174357, 91421303, 11527806, 11434003, 11374057, and 11421404, and by the Strategic Priority Research Program B of the Chinese Academy of Sciences Grant No. XDB07010100.

J.W. and X.G. contributed equally to this work.

[1] D. Fay and J. Appel, Phys. Rev. B **22**, 3173 (1980).

[2] S. R. Julian, Physics **5**, 17 (2012).

[3] T. Hattori, Y. Ihara, Y. Nakai, K. Ishida, Y. Tada, S. Fujimoto, N. Kawakami, E. Osaki, K. Deguchi, N. K. Sato, and I. Satoh, Phys. Rev. Lett. **108**, 066403 (2012).

[4] K. Machida and T. Ohmi, Phys. Rev. Lett. **86**, 850 (2001).

[5] D. V. Shopova and D. I. Uzunov, Phys. Rev. B **72**, 024531 (2005).

[6] S. Saxena, P. Agarwal, K. Ahilan, F. M. Grosche, R. K. W. Haselwimmer, M. J. Steiner, E. Pugh, I. R. Walker, S. R. Julian, and P. Monthoux, Nature (London) **406**, 587 (2000).

[7] D. Aoki, A. Huxley, E. Ressouche, D. Braithwaite, J. Flouquet, J. P. Brison, E. Lhotel, and C. Paulsen, Nature (London) **413**, 613 (2001).
[8] N. T. Huy, A. Gasparini, D. E. de Nijs, Y. Huang, J. C. P. Klaasse, T. Gortenmulder, A. de Visser, A. Hamann, T. Gorlach, and H. von Lohneysen, Phys. Rev. Lett. **99**, 067006 (2007).
[9] F. S. Bergeret, A. F. Volkov, and K. B. Efetov, Phys. Rev. Lett. **86**, 4096 (2001).
[10] A. Kadigrobov, R. I. Shekhter, and M. Jonson, Europhys. Lett. **54**, 394 (2001).
[11] S. R. Keizer, S. T. B. Goennenwein, T. M. Klapwijk, G. X. Miao, G. Xiao, and A. Gupta, Nature (London) **439**, 825 (2006).
[12] M. Sigrist and K. Kazuo, Rev. Mod. Phys. **63**, 239 (1991).
[13] A. P. Mackenzie and Y. Maeno, Rev. Mod. Phys. **75**, 657 (2003).
[14] Y. Maeno, S. Kittaka, T. Nomura, S. Yonezawa, and K. Ishida, J. Phys. Soc. Jpn. **81**, 011009 (2012).
[15] K. D. Nelson, Z. Q. Mao, Y. Maeno, and Y. Liu, Science **306**, 1151 (2004).
[16] F. Kidwingira, J. D. Strand, D. J. Van Harlingen, and Y. Maeno, Science **314**, 1267 (2006).
[17] A. Bouhon and M. Sigrist, New J. Phys. **12**, 043031 (2010).
[18] J. Jang, D. G. Ferguson, V. Vakaryuk, R. Budakian, S. B. Chung, P. M. Goldbart, and Y. Maeno, Science **331**, 186 (2011).
[19] P. G. Björnsson, Y. Maeno, M. E. Huber, and K. A. Moler, Phys. Rev. B **72**, 012504 (2005).
[20] J. R. Kirtley, C. Kallin, C. W. Hicks, E. A. Kim, Y. Liu, K. A. Moler, Y. Maeno, and K. D. Nelson, Phys. Rev. B **76**, 014526 (2007).
[21] C. W. Hicks, J. R. Kirtley, T. M. Lippman, N. C. Koshnick, M. E. Huber, Y. Maeno, W. M. Yuhasz, M. B. Maple, and K. A. Moler, Phys. Rev. B **81**, 214501 (2010).
[22] J. S. Moodera and R. Meservey, Phys. Rev. B **42**, 179 (1990).
[23] P. LeClair, J. S. Moodera, J. Philip, and D. Heiman, Phys. Rev. Lett. **94**, 037006 (2005).
[24] X. X. Gong, H. X. Zhou, P. C. Xu, D. Yue, K. Zhu, X. F. Jin, H. Tian, G. J. Zhao, and T. Y. Chen, Chin. Phys. Lett. **32**, 067402 (2015).
[25] X. X. Gong, M. Kargarian, A. Stern, D. Yue, H. X. Zhou, X. F. Jin, V. M. Galitski, V. M. Yakovenko, and J. Xia, Sci. Adv. **3**, e1602579 (2017).
[26] M. Sigrist, T. M. Rice, and K. Ueda, Phys. Rev. Lett. **63**, 1727 (1989).
[27] See Supplemental Material at http://link.aps.org/supplemental/10.1103/PhysRevB.96.054519 for more data and discussions.
[28] A. Barone, *Physics and Application of the Josephson Effect* (John Wiley and Sons, Inc., New York, 1982).